Measurement errors resulted from misalignment errors of the retarder in a rotating-retarder complete Stokes polarimeter

Hu Dai[1,2,*] and Changxiang Yan[1]

[1]*Changchun Institute of Optics, Fine Mechanics and Physics, Chinese Academy of Sciences, Changchun 130033, China*
[2]*Graduate School of Chinese Academy of Sciences, Beijing 100039, China*
*daihulove1@126.com

Abstract: Rotatable retarder fixed polarizer (RRFP) Stokes polarimeters, which employ uniformly spaced angles over 180° or 360°, are most commonly used to detect the state of polarization (SOP) of an electromagnetic (EM) wave. The misalignment error of the retarder is one of the major error sources. We suppose that the misalignment errors of the retarder obey a uniform normal distribution and are independent of each other. Then, we derive analytically the covariance matrices of the measurement errors. Based on the covariance matrices derived, we can conclude that 1) the measurement errors are independent of the incident intensity s_0, but seriously depend on the Stokes parameters (s_1, s_2, s_3) and the retardance of the retarder δ; 2) for any mean incident SOP, the optimal initial angle and retardance to minimize the measurement error both can be achieved; 3) when $N = 5$, 10, 12, the initial orienting angle could be used as an added degree of freedom to strengthen the immunity of RRFP Stokes polarimeters to the misalignment error. Finally, a series of simulations are performed to verify these theoretical results.

OCIS codes: (120.5410) Polarimetry; (120.2130) Ellipsometry and polarimetry; (110.5405) Polarimetric imaging; (280.4991) Passive remote sensing.

References and links

1. N. Ghosh and I. A. Vitkin, "Tissue polarimetry: concepts, challenges, applications, and outlook," J. Biomed. Opt. **16**(11), 110801 (2011).
2. A. M. Gandorfer, H. P. Povel, P. Steiner, F. Aebersold, U. Egger, A. Feller, D. Gisler, S. Hagenbuch, and J. O. Stenflo, "Solar polarimetry in the near UV with the Zurich Imaging Polarimeter ZIMPOL II," A&A. **422**(2), 703–708 (2004).
3. J. S. Tyo and T. S. Turner, "Imaging spectropolarimeters for use in visible and infrared remote sensing," in *Imaging Spectrometry V*, M. R. Descour and S. S. Shen, eds., Proc. SPIE **3753**, 214–225 (1999).
4. J. S. Tyo, D. L. Goldstein, D. B. Chenault, and J. A. Shaw, "Review of passive imaging polarimetry for remote sensing applications," Appl. Opt. **45**(22), 5453–5469 (2006).
5. D. H. Goldstein, "Mueller matrix dual-rotating retarder polarimeter," Appl. Opt. **31**(31), 6676–6683 (1992).
6. E. Tandberg-Hanssen, C. C. Cheng, B. E. Woodgate, J. C. Brandt, R. D. Chapman, P. J. Kenney, A. G. Michalitsianos, R. A. Shine, R. G. Athay, J. M. Beckers, E. C. Bruner, R. A. Rehse, S. A. Schoolman, J. B. Gurman, C. L. Hyder, and W. Henze, "Solar maximum mission experiment: Ultraviolet spectroscopy and polarimetry on the solar maximum mission," Adv. Space Res. **1**(13), 275–283 (1981).
7. D. S. Sabatke, M. R. Descour, E. L. Dereniak, W. C. Sweatt, S. A. Kemme, and G. S. Phipps, "Optimization of retardance for a complete Stokes polarimeter," Opt. Lett. **25**(11), 802–804 (2000).
8. J. S. Tyo, "Design of optimal polarimeters: maximization of signal-to-noise ratio and minization of systematic error," Appl. Opt. **41**(4), 619–630 (2002).
9. F. Goudail, "Noise minimization and equalization for Stokes polarimeters in the presence of signal-dependent Poisson shot noise," Opt. Lett. **34**(5), 647–649 (2009).
10. H. Dong, M. Tang, and Y. D. Gong, "Noise properties of uniformly-rotating RRFP Stokes polarimeters," Opt. Express **21**(8), 9674–9690 (2013).
11. J. S. Tyo and H. Wei, "Optimizing imaging polarimeters constructed with imperfect optics," Appl. Opt. **45**(22), 5497–5503 (2006).
12. H. Dong, P. Shum, Y. D. Gong, and Q. Z. Sun, "Measurement errors induced by retardance deviation in a rotatable retarder fixed polarizer Stokes polarimeter," Opt. Eng. **51**(3), 033001 (2012).

#208137 - $15.00 USD Received 12 Mar 2014; revised 3 May 2014; accepted 5 May 2014; published 9 May 2014

13. J. S. Tyo, “Design of optimal polarimeters: maximization of signal-to-noise ratio and minimization of systematic error,” Appl. Opt. **41**(4), 619–630 (2002).
14. D. S. Sabatke, A. M. Locke, M. R. Descour, W. C. Sweatt, J. P. Garcia, E. L. Dereniak, S. A. Kemme, and G. S. Phipps, “Figures of merit for complete Stokes polarimeter optimization,” in *Proceedings of Polarization: Measurement, Analysis, and Remote Sensing III*, D. B. Chenault, eds., Proc. SPIE **4133** (2000).

1. Introduction

Measurement of the state of polarization (SOP) of an electromagnetic (EM) wave is attracting more and more attention because it plays an important role in many regions, such as biomedicine [1], solar astronomy [2] and remote sensing [3]. The Stokes vector is a widely accepted means to describe the SOP of an incident EM wave. The simplest complete Stokes polarimeter is a rotatable retarder fixed polarizer (RRFP) Stokes polarimeter with a rotatable retarder, a fixed polarizer and a photodetector, which is shown in Fig. 1. Often, a quarter-wave retarder is chosen in a commercial polarimeter. Its structure is simple, thus a RRFP Stokes polarimeter can be easily integrated in many application systems, such as imaging polarimeters [4], Mueller matrix polarimeters [5] and solar polarimetric telescopes [6].

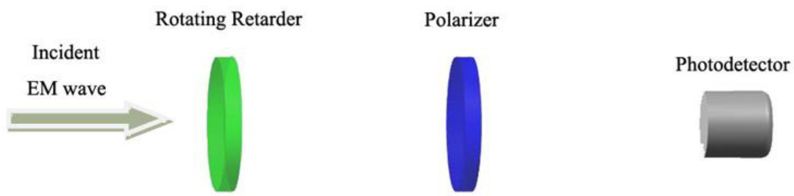

Fig. 1. The schematic structure of a RRFP Stokes polarimeter.

A RRFP Stokes polarimeter determines the four Stokes parameters of an incident EM wave by rotating the retarder to N ($N \geq 4$) different angular orientations and measuring the corresponding optical intensities of the EM wave. There are three potential error sources in such measurements: first, the random noise in the measured intensity; second, deviations in nominal values of retardance and diattenuation of the polarization optics; and third, the relative angular orientation errors away from the nominal angular orientations. These three error sources introduce Stokes parameter errors because they all induce errors in the measured intensity of the incident EM wave.

The first two error sources have been systematically investigated. The noise properties of RRFP Stokes polarimeters in the presence of Gaussian noise were theoretically investigated by Sabatke and Tyo [7, 8]. They found that a 132° retarder and an angle set of (−51.7°, −15.1°, 15.1°, 51.7°) can result in the largest SNR for the system. Moreover, Sabatke found that uniformly spaced angles over 360° are a good choice, and the practical difficulty and time expenditure of aligning the retarder at many different non-uniformly spaced angles is unnecessary [7]. Goudail looked at signal-dependent shot noise, and found that in a certain circumstance, the polarimeters optimal for Gaussian noise are also optimal for signal-dependent shot noise [9]. H. Dong (2013) investigated the measurement noises of Stokes parameters resulted from photodetector noises in RRFP Stokes polarimeters employing uniformly spaced angles over 180° or 360° by theoretical analysis and simulation [10]. For the second source of error, such as retarder non-uniformity and low extinction ratio of a linear polarizer, Tyo and Wei had determined that a low extinction ratio of a linear polarizer did not depress the signal-to-noise ratio [11]. H. Dong (2012) studied measurement errors induced by retardance deviation and derived theoretically the relationship between the retarance error and the measurement errors in RRFP Stokes polarimeters [12].

However, the above mentioned studies all assumed that the optical intensities were measured at the ideal retarder orientation angles. In practice, there will be angular orientation errors of the retarder during the procedure of measurement. Further, angular orientation error is far more important in a RRFP imaging polarimeter [11]. Tyo studied the sensitivity of polarimeters to this kind of error source analytically, and discussed the relationship between system condition and error minimization by means of numerical analysis [13]. But the analytical result presented in [13] can only be used for the case that the incident SOPs are uniformly distributed over the Poincaré sphere.

In this paper, we address the third error source of RRFP Stokes polarimeters measuring intensities in N ($N\geq5$) uniformly spaced angles by theoretical analysis and simulation. The retarder misalignment errors are treated as statistic errors, and the covariance matrices of measurement errors induced by the retarder misalignment errors are derived analytically. Based on the covariance matrices, it can be concluded that 1) the measurement errors from the retarder misalignment errors are independent of the incident intensity s_0, but being dependent on Stokes parameters s_1, s_2, s_3 under test; 2) for any incident SOP, the optimal configuration of a RRFP polarimeter including the initial angle and the retardance can be achieved; 3) for the case of $N = 5$, 10, 12, the effect of the retarder misalignment error has been remarkably weakened when an initial angle leading to the smallest WS is used; 4) the covariance matrix for N uniformly spaced angles over 180° has the same form as that for $2N$ uniformly spaced angles over 360°. In the end of the paper, simulations are performed to verify that these theoretical results agree well with the simulation results.

2. Theoretical analysis

RRFP Stokes polarimeters determine the Stokes vector $\vec{\mathbf{S}}$ of an incident EM wave by obtaining N ($N\geq4$) intensity measurements $\vec{\mathbf{I}} = (I_0, I_1, \cdots, I_N)^T$ corresponding to N angular orientations of the retarder. Without any errors, the two vectors are related by

$$\vec{\mathbf{I}} = \mathbf{W}\vec{\mathbf{S}} \tag{1}$$

$$\mathbf{W} = \frac{1}{2}\begin{pmatrix} 1 & \cos^2 2\theta_1 + \cos\delta \sin^2 2\theta_1 & \sin^2(\delta/2)\sin 4\theta_1 & -\sin\delta\sin 2\theta_1 \\ 1 & \cos^2 2\theta_2 + \cos\delta \sin^2 2\theta_2 & \sin^2(\delta/2)\sin 4\theta_2 & -\sin\delta\sin 2\theta_2 \\ \vdots & \vdots & \vdots & \vdots \\ 1 & \cos^2 2\theta_N + \cos\delta \sin^2 2\theta_N & \sin^2(\delta/2)\sin 4\theta_N & -\sin\delta\sin 2\theta_N \end{pmatrix} \tag{2}$$

where $\mathbf{W}$ is the measurement matrix, $\vec{\mathbf{S}} = (s_0, s_1, s_2, s_3)^{\mathrm{T}}$ is the incident Stokes vector, the superscript "T" denotes the transposition of a vector or a matrix, δ is the retardance of the retarder, $\theta_i = \theta_1 + (i\ 1)360°/N$, ($i = 1, 2, \ldots, N$-1, N) is the nominal angular orientation of the retarder when the intensity I_i is detected, and θ_1 is the initial angular orientation.

When there is only the misalignment error of the retarder, the real measurement matrix of the Stokes polarimeter is denoted by $\mathbf{W'}$. Supposed that $\mathbf{W'} = \mathbf{W} + \Delta\mathbf{W}$, then the measurement error of the intensity induced by the misalignment error of the retarder is governed by

$$\Delta\vec{\mathbf{I}} = \left(\mathbf{W}' - \mathbf{W}\right)\vec{\mathbf{S}} = \Delta\mathbf{W}\vec{\mathbf{S}} \tag{3}$$

when the angular orientation error is small enough, the approximation in Eq. (4) which is the first term of a Taylor-series expansion of $\mathbf{W}_{ij}$ about the nominal settings is appropriate:

$$\Delta\mathbf{W}_{ij} = \mathbf{W'}_{ij} - \mathbf{W}_{ij} = \xi_i\left[\frac{\mathbf{W}_{ij}(\theta_i + \xi_i) - \mathbf{W}_{ij}(\theta_i)}{\xi_i}\right] \approx \xi_i \frac{\partial\mathbf{W}_{ij}(\theta)}{\partial\theta}\Big|_{\theta_i} \tag{4}$$

#208137 - $15.00 USD Received 12 Mar 2014; revised 3 May 2014; accepted 5 May 2014; published 9 May 2014

where ξ_i is the angular orientation error of the retarder for the *i*th measurement. When the error ξ_i is less than 0.05 rad, the truncation error from the approximation in Eq. (4) is under 1%. Consequently, the matrix $\Delta\mathbf{W}$ is obtained by

$$\Delta\mathbf{W}=\begin{pmatrix} 0 & \sin 4\theta_1(\cos\delta-1)\xi_1 & -\cos 4\theta_1(\cos\delta-1)\xi_1 & -\cos 2\theta_1\sin\delta\xi_1 \\ 0 & \sin 4\theta_2(\cos\delta-1)\xi_2 & -\cos 4\theta_2(\cos\delta-1)\xi_2 & -\cos 2\theta_2\sin\delta\xi_2 \\ \vdots & \vdots & \vdots & \vdots \\ 0 & \sin 4\theta_N(\cos\delta-1)\xi_N & -\cos 4\theta_N(\cos\delta-1)\xi_N & -\cos 2\theta_N\sin\delta\xi_N \end{pmatrix} \quad (5)$$

To obtain the relationship between the intensity error $\Delta\vec{\mathbf{I}}$ and the angular orientation error $\vec{\boldsymbol{\xi}}$, Eq. (3) is transformed as

$$\Delta\vec{\mathbf{I}}=\mathbf{Q}\vec{\boldsymbol{\xi}} \quad (6)$$

where $\mathbf{Q}$ is the transforming matrix, its elements are given by

$$\mathbf{Q}_{ij}=\begin{cases} s_1\sin 4\theta_i(\cos\delta-1)-s_2\cos 4\theta_i(\cos\delta-1)-s_3\cos 2\theta_i\sin\delta, & i=j; \\ 0 & , i\neq j. \end{cases} \quad (7)$$

and $\vec{\boldsymbol{\xi}}=(\xi_1,\xi_2\cdots\xi_N)^{\mathrm{T}}$ is the angular orientation error vector of the retarder in a RRFP Stokes polarimeter. Hence, the Stokes error vector from the angular orientation error can be derived as

$$\vec{\in}=\mathbf{W}^{+}\Delta\vec{\mathbf{I}}=\left(\mathbf{W}^{\mathrm{T}}\mathbf{W}\right)^{-1}\mathbf{W}^{\mathrm{T}}\mathbf{Q}\vec{\boldsymbol{\xi}} \quad (8)$$

where $\mathbf{W}^{+}$ is the pseudo inverse matrix, which is defined by

$$\mathbf{W}^{+}=\left(\mathbf{W}^{\mathrm{T}}\mathbf{W}\right)^{-1}\mathbf{W}^{\mathrm{T}} \quad (9)$$

and the superscript "-1" denotes the inverse of a square matrix. It is obvious that by Eq. (8), the error propagation relationship from the angular orientation error to the Stokes error is obtained. Note that the result that is similar to Eq. (8) is also presented by Tyo in [13].

When a RRFP Stokes polarimeter is operating, the retarder is rotated harmonically to modulate the incident EM wave. The angular orientation errors of the retarder arise from the following factors: 1) the initial angle deviation from the nominal value θ_1; 2) non-harmonic rotation of the retarder; 3) non-uniform time intervals of intensity measurements. The sources of these kinds of errors are so varied that the angular orientation errors of the retarder are assumed to be independent of each other and obey a uniform normal distribution to simplify the analysis, and the standard deviation of the distribution is σ. Based on this assumption, the measurement error of the Stokes vector $\vec{\in}$ consists of four random variables, and their variances are usually used to assess the measurement errors of Stokes parameters [7, 14]. From Eq. (8), the covariance matrix on Stokes parameters can be derived as

$$\boldsymbol{\Gamma}_{\in}=\left\langle \vec{\in}\vec{\in}^{\mathrm{T}}\right\rangle=\begin{pmatrix} \langle\in_0^2\rangle & \langle\in_0\in_1\rangle & \langle\in_0\in_2\rangle & \langle\in_0\in_3\rangle \\ \langle\in_1\in_0\rangle & \langle\in_1^2\rangle & \langle\in_1\in_2\rangle & \langle\in_1\in_2\rangle \\ \langle\in_2\in_0\rangle & \langle\in_2\in_1\rangle & \langle\in_2^2\rangle & \langle\in_2\in_3\rangle \\ \langle\in_3\in_0\rangle & \langle\in_3\in_1\rangle & \langle\in_3\in_2\rangle & \langle\in_3^2\rangle \end{pmatrix}=\left(\mathbf{W}^{\mathrm{T}}\mathbf{W}\right)^{-1}\mathbf{W}^{\mathrm{T}}\mathbf{Q}\left\langle\vec{\boldsymbol{\xi}}\vec{\boldsymbol{\xi}}^{\mathrm{T}}\right\rangle\mathbf{Q}^{\mathrm{T}}\mathbf{W}\left(\mathbf{W}^{\mathrm{T}}\mathbf{W}\right)^{-1} \quad (10)$$

#208137 - $15.00 USD Received 12 Mar 2014; revised 3 May 2014; accepted 5 May 2014; published 9 May 2014

where the <·> operator indicates the expectation value. Since we have assumed that the elements of the angular orientation error $\vec{\boldsymbol{\xi}}$ are independent of each other with a uniform standard variance σ, the covariance matrix in Eq. (10) can be expressed as

$$\boldsymbol{\Gamma}_{\epsilon} = \sigma^2 \left(\mathbf{W}^{\mathrm{T}}\mathbf{W}\right)^{-1} \boldsymbol{\Lambda} \left(\mathbf{W}^{\mathrm{T}}\mathbf{W}\right)^{-1} = \sigma^2 \boldsymbol{\Gamma} \tag{11}$$

where the matrix **Λ** is

$$\boldsymbol{\Lambda} = \mathbf{W}^{\mathbf{T}}\mathbf{Q}\left(\mathbf{W}^{\mathbf{T}}\mathbf{Q}\right)^{\mathbf{T}} \tag{12}$$

and the matrix **Γ** is

$$\boldsymbol{\Gamma} = \left(\mathbf{W}^{\mathrm{T}}\mathbf{W}\right)^{-1} \boldsymbol{\Lambda} \left(\mathbf{W}^{\mathrm{T}}\mathbf{W}\right)^{-1} \tag{13}$$

when N uniformly spaced angles θ_1, θ_1 + 360°/N,…, θ_1 + (N-1)360°/N (N≥5) are used, the matrix $\left(\mathbf{W}^{\mathrm{T}}\mathbf{W}\right)^{-1}$ can be given by

$$\left(\mathbf{W}^{\mathrm{T}}\mathbf{W}\right)^{-1} = \frac{4}{N}\begin{pmatrix} \frac{3+2\cos\delta+3\cos^2\delta}{(1-\cos\delta)^2} & -\frac{4(1+\cos\delta)}{(1-\cos\delta)^2} & 0 & 0 \\ -\frac{4(1+\cos\delta)}{(1-\cos\delta)^2} & \frac{8}{(1-\cos\delta)^2} & 0 & 0 \\ 0 & 0 & \frac{8}{(1-\cos\delta)^2} & 0 \\ 0 & 0 & 0 & \frac{2}{\sin^2\delta} \end{pmatrix} \tag{14}$$

when N uniformly spaced angles θ_1, θ_1 + 360°/N, …, θ_1 + (N-1)360°/N (N = 9, 11, 13, 15, 17, 18, 19 …∞), the matrix **Λ** can be given by

#208137 - $15.00 USD Received 12 Mar 2014; revised 3 May 2014; accepted 5 May 2014; published 9 May 2014

$$
\begin{cases}
\Lambda_{11} = \frac{N}{8}\left[s_1^2 (\cos\delta - 1)^2 + s_2^2 (\cos\delta - 1)^2 + s_3^2 \sin^2\delta \right] \\
\Lambda_{12} = \Lambda_{21} = \frac{N}{16} s_1^2 \sin^2\delta (1-\cos\delta) + \frac{N}{16} s_2^2 \sin^2\delta (1-\cos\delta) \\
\qquad + \frac{N}{32} s_3^2 (3+\cos\delta)\sin^2\delta \\
\Lambda_{13} = \Lambda_{31} = \Lambda_{34} = \Lambda_{43} = 0 \\
\Lambda_{14} = \Lambda_{41} = \frac{N}{8} s_1 s_3 \sin^2\delta (\cos\delta - 1) \\
\Lambda_{22} = \frac{N}{128} s_1^2 (\cos\delta-1)^2 (5+6\cos\delta+5\cos^2\delta) + \frac{N}{128} s_2^2 (\cos\delta-1)^2 (7+2\cos\delta+7\cos^2\delta) \\
\qquad + \frac{N}{64} s_3^2 \sin^2\delta (5+2\cos\delta+\cos^2\delta) \\
\Lambda_{23} = \Lambda_{32} = \frac{N}{32} s_1 s_2 (\cos\delta-1)^3 \sin^2\frac{\delta}{2} \\
\Lambda_{24} = \Lambda_{42} = -\frac{N}{16} s_1 s_2 \sin^4\delta \\
\Lambda_{33} = \frac{3N}{32} s_1^2 (\cos\delta-1)^2 \sin^4\frac{\delta}{2} + \frac{N}{32} s_2^2 (\cos\delta-1)^2 \sin^4\frac{\delta}{2} + \frac{N}{16} s_3^2 \sin^2\delta \sin^4\frac{\delta}{2} \\
\Lambda_{44} = \frac{N}{16} s_1^2 (\cos\delta-1)^2 \sin^2\delta + \frac{N}{16} s_2^2 (\cos\delta-1)^2 \sin^2\delta + \frac{N}{32} s_3^2 \sin^4\delta
\end{cases} \tag{15}
$$

During the procedure of deriving Eq. (14) and Eq. (15), lots of trigonometric identities are used, which all have been validated by MATLAB programs. From Eq. (11), Eq. (14) and Eq. (15), when N uniformly spaced angles θ_1, $\theta_1 + 360°/N$, …, $\theta_1 + (N\text{-}1)360°/N$ (N = 9, 11, 13, 15, 17, 18, 19, …,∞) are used, the matrix $\mathbf{\Gamma}$ can be given by

$$
\begin{cases}
\Gamma_{11} = \frac{4}{N} s_1^2 (1+\cos^2\delta) + \frac{8}{N} s_2^2 (1+\cos\delta+\cos^2\delta) - \frac{2}{N} s_3^2 \frac{(5\cos^3\delta + 7\cos^2\delta + 3\cos\delta + 1)}{(\cos\delta - 1)} \\
\Gamma_{22} = \frac{8}{N} s_1^2 + \frac{24}{N} s_2^2 + \frac{16}{N} s_3^2 \cot^2\frac{\delta}{2} \\
\Gamma_{33} = \frac{24}{N} s_1^2 + \frac{8}{N} s_2^2 + \frac{16}{N} s_3^2 \cot^2\frac{\delta}{2} \\
\Gamma_{44} = \frac{4}{N} s_1^2 \tan^2\frac{\delta}{2} + \frac{4}{N} s_2^2 \tan^2\frac{\delta}{2} + \frac{2}{N} s_3^2
\end{cases} \tag{16}
$$

From Eq. (11), the matrix $\mathbf{\Gamma}$ is independent of the alignment error of the retarder. Its diagonal elements represent gain factors in the propagation of variance from the measurements to the Stokes vector estimate. The off-diagonal elements indicate where correlations in errors in the components of the Stokes vector estimate arise [14], which have been derived, but are not shown here because they won't be used in this paper. The diagonal elements of the covariance matrix $\mathbf{\Gamma}_\in$ denote the corresponding measurement errors of the four Stokes parameters. So the sum of four measurement errors of Stokes parameters $\sum_{i=0}^{3}\langle \in_i^2 \rangle$, which is equal to the trace of the covariance matrix $\mathbf{\Gamma}_\in$, can be used to evaluate the overall measurement error induced by angular orientation errors of the retarder. Based on Eq. (16), it is given as

$$\sum_{i=0}^{3} \epsilon_i^{\,2} = Tr\left(\mathbf{\Gamma}_{\epsilon}\right) = \frac{4\sigma^2}{N}\left(C_1 s_1^{\,2} + C_2 s_2^{\,2} + C_3 s_3^{\,2} + C_4 s_1 s_2 + C_5 s_2 s_3 + C_6 s_1 s_3\right) \quad (17)$$

when $N = 9, 11, 13, 15, 17, 18, 19 \ldots \infty$, the six coefficients are respectively

$$\begin{cases} C_1 = \dfrac{\cos^4\delta + 7\cos^2 + 2\cos\delta - 10}{\cos^2\delta - 1}, \\ C_2 = \dfrac{2\cos^4\delta + 2\cos^3\delta + 7\cos^2\delta - 11}{\cos^2\delta - 1}, \\ C_3 = -\dfrac{5\cos^4\delta + 12\cos^3\delta + 25\cos^2\delta + 36\cos\delta + 18}{2\left(\cos^2\delta - 1\right)}, \\ C_4 = C_5 = C_6 = 0 \end{cases} \quad (18)$$

From Eq. (17), it is concluded that the measurement error induced by the angular orientation of retarder is independent of the incident intensity s_0, but seriously depends on the incident Stokes parameters (s_1, s_2, s_3) and the retardance δ. The measurement error is also inversely proportional to N, which agrees well with the prediction in [8]. With the number of intensity measurement N increasing, the measurement error decreases rapidly. But when N exceeds some value, the change will not be obvious any more. Since the polarization degree of an EM wave is defined by Eq. (19), we can conclude that for the case of $N = 9, 11, 13, 15, 17, 18, 19 \ldots\infty$, the higher the polarization degree of an incident EM wave is, the larger the measurement error is.

$$PD = \frac{\sqrt{s_1^{\,2} + s_2^{\,2} + s_3^{\,2}}}{s_0} \quad (19)$$

The coefficients C_1, C_2, C_3, C_4, C_5 and C_6 can be seen as weights of contributions of Stokes parameters (s_1, s_2, s_3) to the measurement error. The coefficients C_1, C_2 and C_4 denote the dependence of the measurement error on the linear polarized component in the incident EM wave. The third coefficient C_3 represents the dependence on the circular polarized component. The coefficients C_5 and C_6 indicate the dependence on the elliptical polarized component. The weight factors C_1, C_2, C_3 for the case of $N = 9, 11, 13, 15, 17, 18, 19 \ldots \infty$ are plotted in Fig. 2. Based on Fig. 2, it is found that when the incident SOPs are mostly distributed near the equator of the Poincaré sphere, in order to minimize the measurement error, the retardance of the retarder should not be larger than 130°. For example, the quarter-wave retarder is a good choice in this instance. When the incident SOPs are mostly distributed over the two poles of the Poincaré sphere, the retardance of the retarder should not be smaller than 85°.

#208137 - $15.00 USD Received 12 Mar 2014; revised 3 May 2014; accepted 5 May 2014; published 9 May 2014

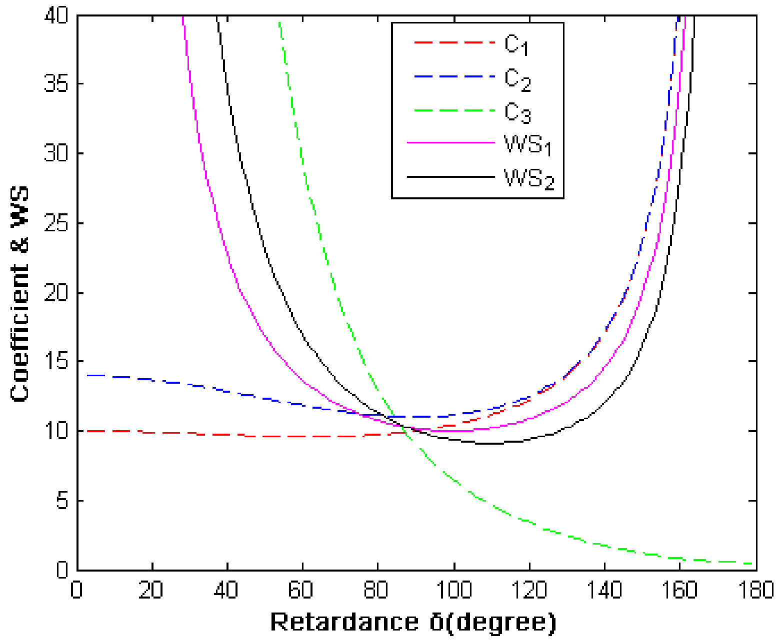

Fig. 2. The relationships between C_1, C_2, C_3, WS_1, WS_2 and the retardance δ for the case of employing N (N = 9, 11, 13, 15, 17, 18, 19…∞) uniformly spaced angles over 360°.

If the statistic distribution of the incident SOPs under test can be theoretically predicted or be known from the previous data, a figure of merit, which is based on the weights on the importance of the respective Stokes components to the polarimeter's intended application, can be designed by composing a weight sum of the six coefficients C_1, C_2, C_3, C_4, C_5 and C_6 to evaluate the measurement error. The figure of merit is defined as the Weight Sum (WS) by Eq. (20).

$$WS = \overline{s_1}^2 C_1 + \overline{s_2}^2 C_2 + \overline{s_3}^2 C_3 + \overline{s_1 s_2} C_4 + \overline{s_2 s_3} C_5 + \overline{s_1 s_3} C_6 \tag{20}$$

where $\left(1, \overline{s_1}, \overline{s_2}, \overline{s_3}\right)^{\mathrm{T}}$ is the normalized mean incident Stokes vector under test. In this case, an optimal value of the retardance resulting in the smallest WS can be achieved to minimize the measurement error. For example, when the mean distribution of incident SOPs is evaluated as $\left(1, 1/\sqrt{2}, 1/\sqrt{3}, 1/\sqrt{6}\right)^{\mathbf{T}}$, the figure of merit WS_1 is given by

$$WS_1 = \frac{C_1}{2} + \frac{C_2}{3} + \frac{C_3}{6} \tag{21}$$

The relationship between WS_1 and the retardance is also shown in Fig. 2. When the retardance δ is 99.42° for the case of N = 9, 11, 13, 15, 17, 18, 19 …∞, the measurement error reaches the minimum. Furthermore, in the retardance range from 92.54° to 107.24°, WS_1 increases only by 1% of its minimum. Hence, a retarder in this retardance range can result in nearly a minimum measurement error for the supposed mean incident SOP.

Again, when incident SOPs are uniformly distributed over the Poincaré sphere, it means that the mean incident SOP is $\left(1, 1/\sqrt{3}, 1/\sqrt{3}, 1/\sqrt{3}\right)^{\mathbf{T}}$. The figure of merit WS_2, which is still shown in Fig. 2, is given by

$$WS_2 = \frac{1}{3}\left(C_1 + C_2 + C_3\right) \tag{22}$$

It can be found that when the retardence δ is 109.68°, the measurement error reaches its minimum. This result is coincident with that obtained by Tyo using Frobenius norm as the figure of merit in [13].

By similar methods to the above, it can be obtained that when $N = 5, 7, 10, 12, 14, 16$, the matrix $\mathbf{\Lambda}$ is a function matrix of the initial angle θ_1. So the covariance matrix $\mathbf{\Gamma}_\in$ is also a function matrix of the initial angle θ_1. These analytical results for $N = 5, 7, 10, 12, 14, 16$ will be presented in what follows.

When N ($N = 5, 10$) uniformly spaced angles θ_1, $\theta_1 + 360°/N$, …, $\theta_1 + (N\text{-}1)360°/N$ are used, the corresponding matrix $\mathbf{\Gamma}$ becomes

$$\begin{cases} \Gamma_{11} = \frac{16}{N}s_1^2\left(1+\cos^2\delta\right) + \frac{32}{N}s_2^2\left(\cos^2\delta + \cos\delta + 1\right) - \frac{8}{N}s_3^2\left(15 - \frac{16}{1-\cos\delta} + 12\cos\delta + 5\cos^2\delta\right) \\ \qquad - \frac{16}{N}s_1s_3\sin 10\theta_1 \sin\delta\left(5 - \frac{4}{1-\cos\delta} + 3\cos\delta\right) + \frac{16}{N}s_2s_3\cos 10\theta_1 \sin\delta\left(5 - \frac{4}{1-\cos\delta} + 3\cos\delta\right) \\ \Gamma_{22} = \frac{32}{N}s_1^2 + \frac{96}{N}s_2^2 + \frac{64}{N}s_3^2\frac{1+\cos\delta}{1-\cos\delta} - \frac{64}{N}s_2s_3\frac{\cos 10\theta_1 \sin\delta}{1-\cos\delta} + \frac{64}{N}s_1s_3\frac{\sin 10\theta_1 \sin\delta}{1-\cos\delta} \\ \Gamma_{33} = \frac{96}{N}s_1^2 + \frac{32}{N}s_2^2 + \frac{64}{N}s_3^2\cot^2\frac{\delta}{2} + \frac{64}{N}s_2s_3\cos 10\theta_1 \cot\frac{\delta}{2} - \frac{64}{N}s_1s_3\sin \\ 10\theta_1\cot\frac{\delta}{2} \\ \Gamma_{44} = \frac{16}{N}s_1^2\frac{1-\cos\delta}{1+\cos\delta} + \frac{16}{N}s_2^2\frac{1-\cos\delta}{1+\cos\delta} + \frac{8}{N}s_3^2 - \frac{16}{N}s_1s_3\frac{\sin 10\theta_1 \sin\delta}{1+\cos\delta} + \frac{16}{N}s_2s_3\frac{\cos 10\theta_1 \sin\delta}{1+\cos\delta} \end{cases} \tag{23}$$

when N ($N = 7, 14$) uniformly spaced angles θ_1, $\theta_1 + 360°/N$, …, $\theta_1 + (N\text{-}1)360°/N$ are used, the corresponding matrix $\mathbf{\Gamma}$ becomes

$$\begin{cases} \Gamma_{11} = \frac{4}{N}s_1^2\left(\cos^2\delta + 1\right) + \frac{8}{N}s_2^2\left(\cos^2\delta + \cos\delta + 1\right) + \frac{2}{N}s_3^2\frac{\sin^2\delta\left(5\cos^2\delta + 2\cos\delta + 1\right)}{\left(\cos\delta - 1\right)^2} \\ \qquad + \frac{4}{N}s_2s_3\frac{\cos 14\theta_1 \sin\delta\left(\cos\delta + 1\right)^2}{\cos\delta - 1} - \frac{4}{N}s_1s_3\frac{\sin 14\theta_1 \sin\delta\left(\cos\delta + 1\right)^2}{\cos\delta - 1} \\ \Gamma_{22} = \frac{8}{N}s_1^2 + \frac{24}{N}s_2^2 + \frac{16}{N}s_3^2\frac{1+\cos\delta}{1-\cos\delta} - \frac{16}{N}s_2s_3\frac{\cos 14\theta_1 \sin\delta}{1-\cos\delta} + \frac{16}{N}s_1s_3\frac{\sin 14\theta_1 \sin\delta}{1-\cos\delta} \\ \Gamma_{33} = \frac{24}{N}s_1^2 + \frac{8}{N}s_2^2 + \frac{16}{N}s_3^2\cot^2\frac{\delta}{2} + \frac{16}{N}s_2s_3\cos 14\theta_1\cot\frac{\delta}{2} - \frac{16}{N}s_1s_3\sin 14\theta_1\cot\frac{\delta}{2} \\ \Gamma_{44} = \frac{4}{N}s_1^2\tan^2\frac{\delta}{2} + \frac{4}{N}s_2^2\tan^2\frac{\delta}{2} + \frac{2}{N}s_3^2 \end{cases} \tag{24}$$

when N ($N = 12$) uniformly spaced angles θ_1, $\theta_1 + 360°/N$, …, $\theta_1 + (N\text{-}1)360°/N$ are used, the corresponding matrix $\mathbf{\Gamma}$ becomes

#208137 - $15.00 USD Received 12 Mar 2014; revised 3 May 2014; accepted 5 May 2014; published 9 May 2014

$$\begin{cases} \Gamma_{11} = \dfrac{4}{N}s_1^{\ 2}\left[\cos 12\theta_1 + 1 - \cos^2\delta\left(\cos 12\theta_1 - 1\right)\right] + \dfrac{4}{N}s_2^{\ 2}\left[2 - \cos 12\theta_1 + 2\cos\delta + \cos^2\delta\left(\cos 12\theta_1 + 2\right)\right] \\ \qquad - \dfrac{2}{N}s_3^{\ 2}\left[7\cos 12\theta_1 + 15 + 4\cos\delta\left(\cos 12\theta_1 + 3\right) + \cos^2\delta\left(\cos 12\theta_1 + 5\right) - \dfrac{8\left(\cos 12\theta_1 + 2\right)}{1-\cos\delta}\right] \\ \Gamma_{22} = \dfrac{8}{N}s_1^{\ 2} + \dfrac{24}{N}s_2^{\ 2} + \dfrac{8}{N}s_3^{\ 2}\left(\cos 12\theta_1 + 2\right)\dfrac{1+\cos\delta}{1-\cos\delta} \\ \Gamma_{33} = \dfrac{24}{N}s_1^{\ 2} + \dfrac{8}{N}s_2^{\ 2} + \dfrac{8}{N}s_3^{\ 2}\left(2 - \cos 12\theta_1\right)\cot^2\dfrac{\delta}{2} \\ \Gamma_{44} = \dfrac{2}{N}s_1^{\ 2}\left(\cos 12\theta_1 + 2\right)\dfrac{1-\cos\delta}{1+\cos\delta} - \dfrac{2}{N}s_2^{\ 2}\left(\cos 12\theta_1 - 2\right)\dfrac{1-\cos\delta}{1+\cos\delta} + \dfrac{2}{N}s_3^{\ 2} + \dfrac{4}{N}s_1 s_2 \sin 12\theta_1 \dfrac{1-\cos\delta}{1+\cos\delta} \end{cases} \tag{25}$$

when N (N = 16) uniformly spaced angles θ_1, $\theta_1 + 360°/N$, …, $\theta_1 + (N\text{-}1)360°/N$ are used, the corresponding matrix $\mathbf{\Gamma}$ becomes

$$\begin{cases} \Gamma_{11} = -\dfrac{2}{N}s_1^{\ 2}\left[\cos 16\theta_1 - 2 + 2\cos 16\theta_1\cos\delta + \left(\cos 16\theta_1 - 2\right)\cos^2\delta\right] \\ \qquad + \dfrac{2}{N}s_2^{\ 2}\left[\cos 16\theta_1 + 4 + \left(\cos 16\theta_1 + 2\right)\cos\delta + \left(\cos 16\theta_1 + 4\right)\cos^2\delta\right] \\ \qquad + \dfrac{2}{N}s_3^{\ 2}\left(\dfrac{16}{1-\cos\delta} - 15 - 12\cos\delta - 5\cos^2\delta\right) - \dfrac{4}{N}s_1 s_2 \sin 16\theta_1\left(1+\cos\delta\right)^2 \\ \Gamma_{22} = -\dfrac{8}{N}s_1^{\ 2}\left(\cos 16\theta_1 + 1\right) - \dfrac{8}{N}s_2^{\ 2}\left(\cos 16\theta_1 + 3\right) + \dfrac{16}{N}s_3^{\ 2}\dfrac{1+\cos\delta}{1-\cos\delta} - \dfrac{16}{N}s_1 s_2 \sin 16\theta_1 \\ \Gamma_{33} = \dfrac{8}{N}s_1^{\ 2}\left(1 + \cos 16\theta_1\right) + \dfrac{8}{N}s_2^{\ 2}\left(1 - \cos 16\theta_1\right) + \dfrac{8}{N}s_3^{\ 2}\dfrac{\sin^2\delta}{\left(\cos\delta - 1\right)^2} + \dfrac{16}{N}s_1 s_2 \sin 16\theta_1 \\ \Gamma_{44} = \dfrac{4}{N}s_1^{\ 2}\dfrac{1-\cos\delta}{1+\cos\delta} + \dfrac{4}{N}s_2^{\ 2}\dfrac{1-\cos\delta}{1+\cos\delta} + \dfrac{2}{N}s_3^{\ 2} \end{cases} \tag{26}$$

We find that the covariance matrix for N = 5, 7, 10, 12, 14, 16 is a trigonometric function matrix of the initial angle θ_1, and the period is 360°/N. Though the analytical results for the case of N = 5, 7, 10, 12, 14, 16 are relatively complex, a RRFP Stokes polarimeter, which employs N = 5, 7, 10, 12, 14, 16 intensity measurements, is recommended. That is because that when N = 5, 7, 10, 12, 14, 16, the added degree of freedom by θ_1 can be used to optimize the configuration of a RRFP Stokes polarimeter.

#208137 - $15.00 USD Received 12 Mar 2014; revised 3 May 2014; accepted 5 May 2014; published 9 May 2014

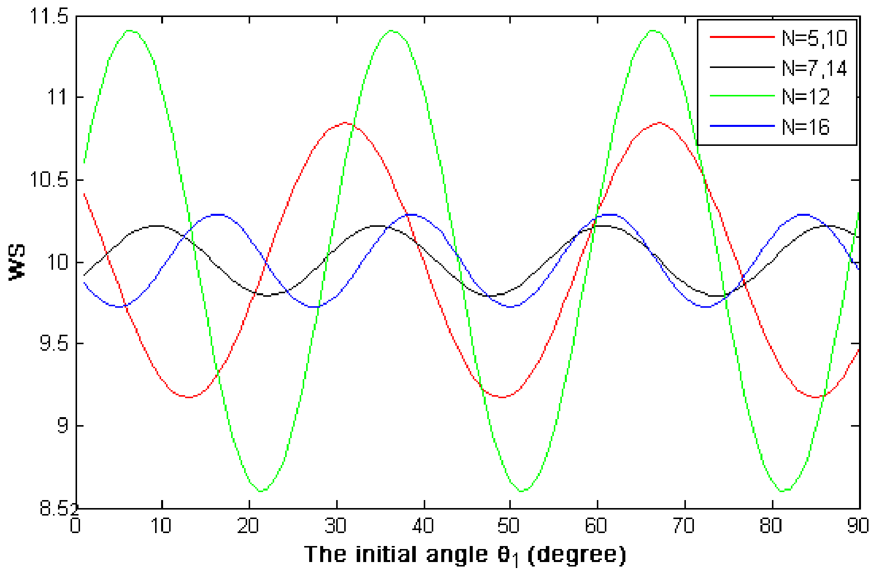

Fig. 3. The relationship between WS and the initial orientation angle θ_1 when $N = 5$ or 10, 7 or 14, 12, 16.

From Eq. (23), Eq. (24), Eq. (25), and Eq. (26), the total measurement error induced by the angular orientation error for the case of $N = 5, 7, 10, 12, 14, 16$ can also be denoted by Eq. (17). Hence, for $N = 5, 7, 10, 12, 14, 16$, the weight sum (WS) of these six corresponding coefficients C_1, C_2, C_3, C_4, C_5, and C_6 can still be used to evaluate the measurement error induced by the misalignment error of the retarder. When the mean incident SOP is assumed as $\left(1, 1/\sqrt{2}, 1/\sqrt{3}, 1/\sqrt{6}\right)^{\mathrm{T}}$, the figure of merit WSs for the case of $N = 5, 7, 10, 12, 14, 16$ are plotted in Fig. 3. It is obvious that the measurement error is a cosine function of the initial angle. As illustrated in Fig. 3, the amplitude for $N = 7, 14, 16$ is too small but that for $N = 5, 10, 12$ is large enough to optimize θ_1. RRFP Stokes polarimeters which use N ($N = 5, 10, 12$) uniformly spaced angles are recommended because an additional parameter of the initial angle θ_1 can be utilized to optimize their configuration. The optimal initial angle for the case of $N = 5$ or 10 is $12.89° + M{\cdot}36°$, while that for the case of $N = 12$ is $21.74° + M{\cdot}30°$. M is an arbitrary positive integer.

When the mean incident SOP is supposed as $\left(1, 1/\sqrt{2}, 1/\sqrt{3}, 1/\sqrt{6}\right)^{\mathrm{T}}$, all of these coefficients and WSs for the case $N = 5$ or 10, 7 or 14, 12, 16 are plotted in Fig. 4. It is not difficult to find that there must be an optimal retardance resulting in the smallest measurement error for all of N. The optimal initial angles and retardances for all of N discussed above are listed in Table 1.

#208137 - $15.00 USD Received 12 Mar 2014; revised 3 May 2014; accepted 5 May 2014; published 9 May 2014

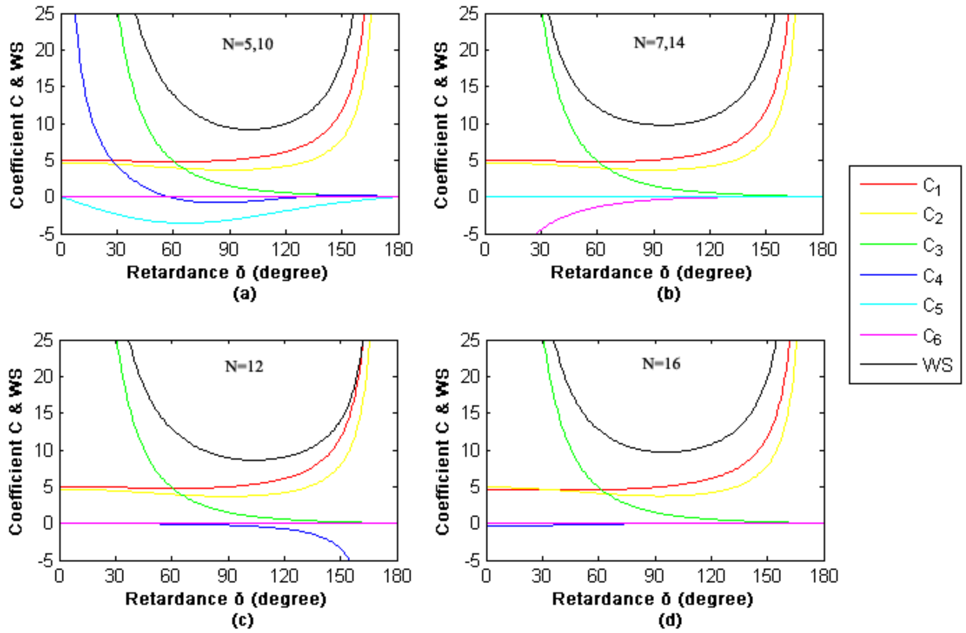

Fig. 4. The coefficients and *WSs* for N = 5 or 10, 7 or 14, 12, 16 at the respective optimal initial angle when the mean incident SOP is $\left(1, 1/\sqrt{2}, 1/\sqrt{3}, 1/\sqrt{6}\right)^{\mathrm{T}}$.

Table 1. Optimal Initial Angle and Retardance for the Incident SOP $\left(1, 1/\sqrt{2}, 1/\sqrt{3}, 1/\sqrt{6}\right)^{\mathrm{T}}$

N	5, 10	7, 14	12	16	9, 11, 13, 15, 17, 18, 19, …, ∞
Optimal initial angle	12.89°	22.23°	21.74°	4.89°	arbitrary value
Optimal retardance	100.58°	95.01°	104.54°	96°	99.42°

In addition, when employing N (N = 4, 6, 8) uniformly spaced angles over 360°, the measurement matrix **W** is a singular matrix. In this case, the RRFP polarimeter cannot determine all of Stokes parameters, which has no practical significance for a generalized RRFP Stokes polarimeter because a RRFP polarimeter is usually used as a complete polarimeter. So the cases of N = 4, 6, 8 are not covered in our discussion.

Although the discussion above is performed for the case of N uniformly spaced angles over 360°, it is easy to prove that the covariance matrix for N uniformly spaced angles over 180° has the same form as that for 2N uniformly spaced angles over 360°. It means that in the case of 180°, N can be any integer larger than 4. Furthermore, the results are different between 180° and 360° only when N is 10, 12, 14 and 16, which are illustrated in Fig. 5. It is observed that when N = 14 and 16, N uniformly spaced angles over 180° are better to minimize the measurement error. When N = 12, 360° is a better choice. There is no quite obvious difference between 180° and 360° for N = 10.

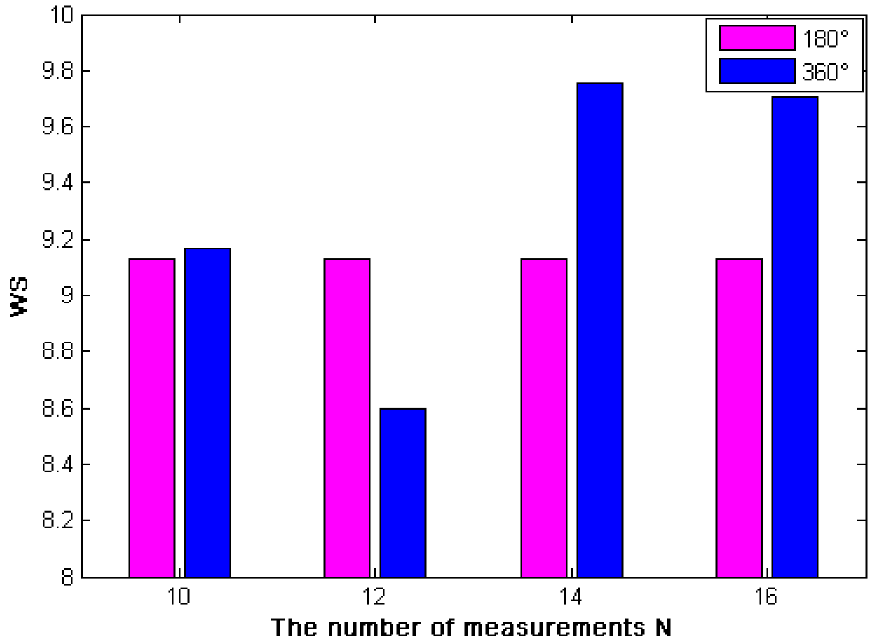

Fig. 5. The comparison of *WS*s for N (N = 10, 12, 14, 16) uniformly spaced angles over between180 °and 360 °.

3. Simulation verification

In order to verify the theoretical results in Eq. (16), Eq. (23), Eq. (24), Eq. (25) and Eq. (26), a series of simulations are performed in this section. These simulations are performed with the following procedures: 1) use MATLAB to generate 10^4 random angular orientation errors, which obey the same normal distribution; 2) calculate the measurement errors with $\vec{\in} = \mathbf{W}^{+}\mathbf{W}\vec{\mathbf{S}} - \vec{\mathbf{S}}$ for each angular orientation error; 3) calculate the variance $\left\langle \in_i^{\,2} \right\rangle$ of the four components of $\vec{\in}$; 4) use Eq. (16), Eq. (23), Eq. (24), Eq. (25) and Eq. (26) to calculate the theoretical result of the corresponding measurement error components. These simulations are carried out in the retardance range from 20° to 160° for 112 different incident SOPs, which are uniformly distributed over the whole Poincaré sphere. Here, only the two typical SOPs $\left(1, 1/\sqrt{3}, 1/\sqrt{3}, 1/\sqrt{3}\right)^{\mathbf{T}}$ and $\left(1, 1/\sqrt{2}, 1/\sqrt{3}, 1/\sqrt{6}\right)^{\mathbf{T}}$ are shown in Fig. 6 and Fig. 7, respectively. The first SOP is measured using an initial angle θ_1 = 9° and σ = 0.05, while the second SOP is measured using an initial angle θ_1 = 13° and σ = 0.02. Both the simulation results and theoretical results are illustrated in the same figure to compare, where the real line "-" represents the simulation result while the star "*" denotes theoretical result. It can be clearly observed that, the theoretical results agree well with the simulation results for the measurement errors of all of the four Stokes parameters for all cases. The small deviation between the two results mostly derives from the truncation error induced by the approximation in Eq. (4).

#208137 - $15.00 USD Received 12 Mar 2014; revised 3 May 2014; accepted 5 May 2014; published 9 May 2014

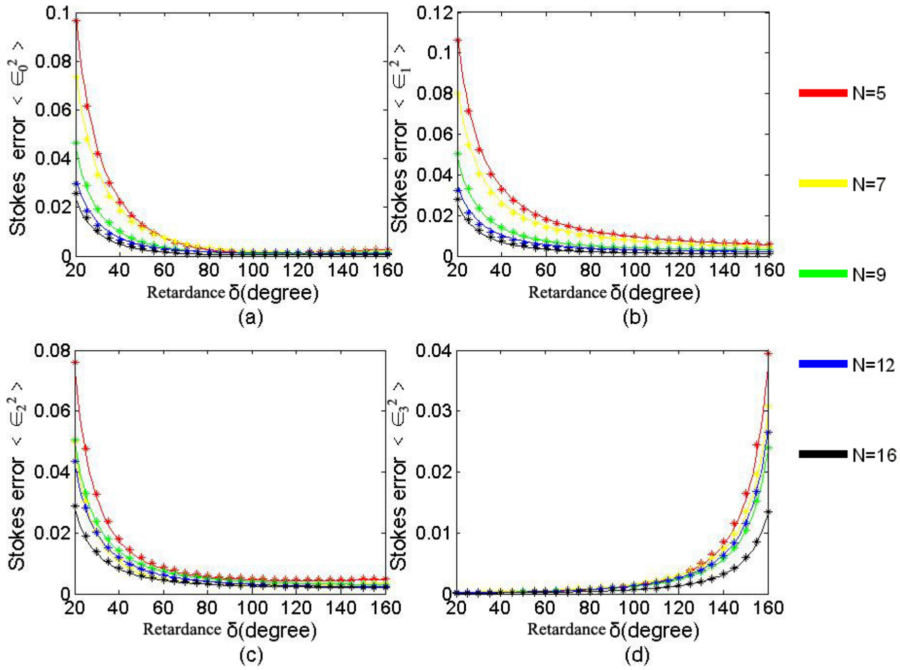

Fig. 6. Simulation and theoretical results of $\left\langle \in_i^2 \right\rangle, i = 0,1,2,3$ at the SOP $\left(1, 1/\sqrt{3}, 1/\sqrt{3}, 1/\sqrt{3}\right)^{\mathrm{T}}$ and the initial angle $\theta_1 = 9^{\circ}$ with σ = 0.05. The real line "-" represents the simulation result while the star "*" denotes theoretical result.

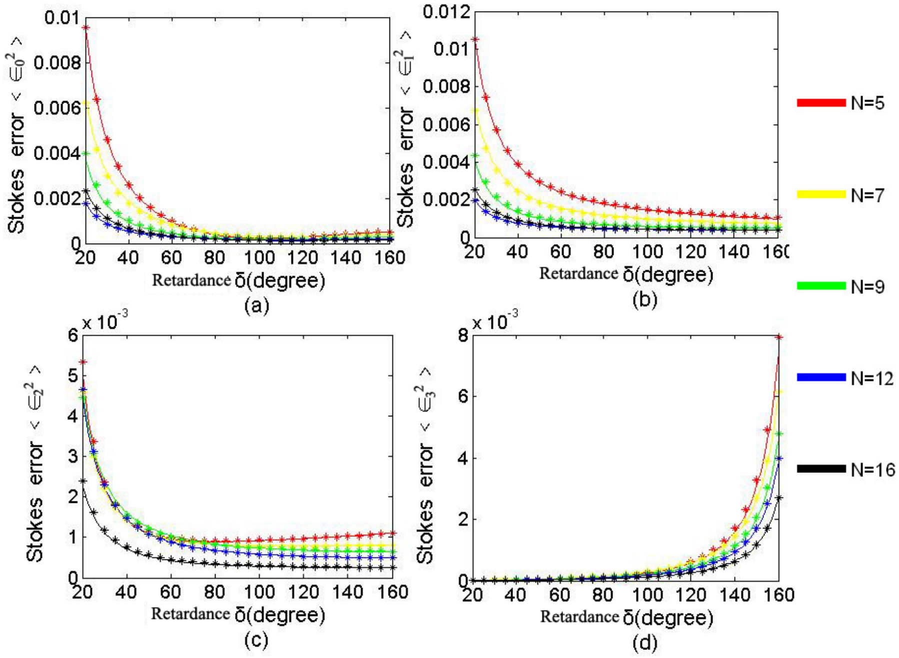

Fig. 7. Simulation and theoretical results of $\langle \in_i^2 \rangle, i = 0, 1, 2, 3$ at the SOP $\left(1, 1/\sqrt{2}, 1/\sqrt{3}, 1/\sqrt{6}\right)^T$ and the initial angle $\theta_1 = 13^\circ$ with σ = 0.02. The real line "-" represents the simulation result while the star "*" denotes theoretical result.

4. Conclusion

For a RRFP Stokes polarimeter, which employs N ($N \geq 5$) uniformly spaced angles over 180° or 360°, the measurement error induced by the angular orientation error of the retarder is investigated by theoretical analysis and verified by simulation. We assume that the angular orientation errors are random variables which obey a uniform normal distribution. The covariance matrices of the measurement errors are derived analytically for the misalignment errors of the retarder. Based on the covariance matrices, we conclude that 1) the measurement errors of Stokes parameters are independent of the incident intensity s_0, but depend heavily on the incident Sstokes parameters (s_1,s_2,s_3) and the retardance of the retarder δ; 2) whatever the incident SOP is, the optimal initial angle and retardance both can be obtained by the analytical results presented above; 3) for the cases of N = 5, 7, 10, 12, 14, 16, the corresponding covariance matrices are different and heavily depend on the initial angle θ_1, and the measurement errors are cosine functions of the initial angle θ_1; 4) the covariance matrix for N uniformly spaced angles over 180° has the same form as that for $2N$ uniformly spaced angles over 360°. Except N = 10, 12, 14, 16, there is nearly no difference between 180° and 360° for the same N. Further, RRFP Stokes polarimeters, which employ N (N = 5 or 10) uniformly spaced angles over 360° or N (N = 5) uniformly spaced angles over 180°, have stronger immunity to the misalignment error of the retarder when the appropriate initial angle is chosen.

Acknowledgment

This work was supported by the National High Technology Research & Development Program of China (Grant NO.2011AA12A103).